Tuijin Jishu/Journal of Propulsion Technology
ISSN: 1001-4055
Vol. 44 No. 4 (2023)

Investigating the Relative Displacement of Ring-Shaped Steel Plate Shear Walls

Farzad Zavari[1], Abdolrahim Jalali[2], Hassan Panahpour[3], Elnaz Alipour[4]

[1] M.S. Earthquake Engineering, Faculty of Civil Engineering, University of Tabriz, Tabriz, Iran

[2] Assistant Professor at Department of Structural Engineering, Faculty of Civil Engineering, University of Tabriz, Iran

[3] Ph.D. student, Faculty of Civil Engineering, University of Tabriz, Tabriz, Iran

[4]Ph.D. Student, Faculty of Erban Planning, Azad University, Tabriz, Iran

Abstract*:* The goal of the present study was to investigate the relative displacement of a ring-shaped steel plate shear wall. To measure the accuracy, efficiency, and validity of the modeling method and analyze the specimens, the present study analyzed the laboratory specimens tested in Natali Egorova's study (2014), using ABAQUS software. Results indicated that the ring-shaped steel plate shear wall could almost remove the effect of pinching in the hysteresis diagram of a simple ring-shaped steel plate shear wall and provide an acceptable hysteresis behavior. It was found that an increase in thickness, a decrease in the ring's radius, an increase in the number of rings, and an increase in the ring's width could increase the strength of the ring-shaped steel plate shear wall. With the increase of thickness, decrease of the ring's radius, increase of the number of rings, increase of the connecting link's width, and increase of the ring's width, the stiffness of the ring-shaped steel plate shear wall also increased. Also, an increase in thickness, a decrease in the width of the connecting link, and an increase in the ring's width helped increase the percentage of energy dissipated. According to this study, software models had fully gone through loading cycles, while laboratory specimens had stopped in some stages of loading under laboratory conditions.

Keywords: ring-shaped steel plate shear wall, hysteresis damping, plate buckling, seismic behavior, finite element model

Introduction

Ring-shaped steel plate shear walls have been studied for a long time, as they have been applied to some structures. Ring-shaped steel plate shear walls, which have been designed and used so far, are mainly developed by thin plates, wherein plane buckling is permissible. Early studies have shown that ring-shaped steel plate shear walls have significant post-buckling capacities, with much energy dissipated when a tensile field is formed. Simple ring-shaped steel plate shear walls are formed of thin sheets surrounded by elements on two lateral (columns) angles, which can be considered as the vertical lateral members, and the elements on the floor (beam) levels, which can be considered horizontal lateral members.

A simple ring-shaped steel plate shear wall is based on an ideal plate to withstand a total base shear. Also, in designing ring-shaped steel plate shear walls, the thickness of a steel plate is determined based on the design force, as lateral elements are so designed to remain in the elastic region before the maximization of the tensile field capacity in the plate. The early buckling of the plate, and consequently, the creation of pinching in the hysteresis curve could cause a sharp reduction in the amount of the dissipated energy and also a sharp loss in the wall's stiffness. Regulations have also proposed moment rigidity connection for these systems to control the stiffness loss and the dissipated energy reduction. However, using moment connections could increase the dimensions of lateral elements and incur more costs in creating ring-shaped steel plate shear walls [1, 2].

To control early buckling and increase stiffness, a plate's thickness has to be increased. The increased plate thickness could increase the force of the tensile field and thus increase the design force of lateral elements, thus increasing the dimensions of lateral components, especially columns.

In 2000, Lubell et al. investigated some experimental single-story and multi-story specimens of an unstiffened ring-shaped steel plate shear wall under quasi-static cyclic loads [3]. Here, a four-story specimen and two single-story specimens were tested. In 1992, Schumacher et al. investigated the behavior of an unstiffened ring-shaped steel plate shear wall at the place where the beam was connected to the column [4]. In 2005, Berman et al. did a test on 6 specimens subjected to cyclic loading [5]. The goal of this study was to compare the cyclic behavior of a ring-shaped steel plate shear wall with a thin plate and a braced frame. The goal was to design a shear wall and a braced frame to both have the necessary lateral strength and to be light enough to be easily used in structures. Analyses suggested that 90% of the initial system's stiffness was due to the presence of the pate in the wall.

In 2011, Chen and Jhang conducted studies on the relationship between the behavior of the steel plate shear wall with low-resisting plates in single- and multi-story frames, concluding that lateral elements created more strength in the frames than the stiffeners, with the buckling strength finally increasing with the decreasing width-to-thickness ratio [6].

In 2008, Stojadinovic and Tipping proposed a type of steel plate shear wall, which used light steel sheets, with lateral elements of the light-frame type being bolted [7]. The findings indicated that in all the specimens, failure at the place of the screws had occurred due to the warping of the plate. Two specimens were added to examine the effect of the addition of corrugated steel plate sheets to both sides of the wall, and it was found that the addition of a two-way wall could double the shear strength. In 2005, Bruneau and Vian carried out tests to investigate the efficiency of a perforated steel plate shear wall, proposing a reduction factor for the computation of strength and the wall's stiffness using several perforations. In 2011, Moghimi and Driver compared the effects of perforations on a steel plate shear wall and a normal shear wall and selected three sets of four-story specimens [8]. Test results also demonstrated that perforations in the wall decreased the shear capacity, though making no changes to the necessary capacity to design columns, as evident in upper floors. This result challenged this type of wall, especially when this feature created some uncertain structural response. Studies by Vian Bruneau (2005) on a specimen with quarter-circle cutouts showed that the cutouts were created in the four corners of the plate, and the main goal of these cutouts was to create accessibility to service infrastructure (e.g., piping, etc.) inside the structures [9].

In 2000, Hitaka et al. conducted tests on steel plate shear walls with slits, with the studied parameters being the rigidity of the beam-to-column connection, strength, and stiffness [10]. The goal of the study was to investigate the reciprocal effects of the frame and plate on each other when they were connected. Three specimen sets were designed, with one case having a beam-to-column connection rigidity percentage larger than 1 and two other cases being smaller than 1. In 2003, Hitaka and Matsui proposed a steel plate shear wall with vertical slits [11]. In this system, the sections between the slits formed moment links, which made the wall have a ductile response. They also proposed relations to compute the initial stiffness of the final strength of the panel with slits.

In 2010, Borchers et al. conducted tests on walls with buckling-resisting channels to reduce buckling in plates with taller links. The behavior of this type of wall was compared to the behavior of walls without these channels [12, 13]. The behavior of these two specimens was identical until the 4% drift. In 2008, Cortest and Liu did tests on slit steel plate shear walls with buckling-resisting channels (Panel BR) [14].

Studies by Borchers et al. (2010) focused on panels with slits and panels with butterfly-shaped fuses [15]. In 2010, Borchers et al. carried out tests on panels with butterfly fuses connected by a backup plate, and the results were compared with those of no-plate specimens [16]. These data indicated that both specimens had identical behavior until the 2.4% drift. In 1985, Tyler did a test on a dissipating tool, used by David Smith and Robert Henry in 1970 [17]. This tool, known as the yielding frame, is used to dissipate energy by the yielding of ring-shaped bars. In 1990, Ciampi and Samuelli-Ferretti proposed pinned steel plates, parallel with yielding frames [18]. These plates had only been designed for axial strength. Thus, plastic deformation in the yielding frame was due to the process of bending. In 2014, Egorova et al. proposed a shear wall, which created rings by cutouts on the sheets of this type of wall, with the rings being diagonally connected by connecting links at 42 ° angles.

This study aimed to examine a ring-shaped steel plate shear wall to be used in practical designs. In this connection, because ring-shaped steel plate walls are considered new ideas, they should be accurately examined to detect their advantages and disadvantages.

Materials and Procedure

As the first step, this study analyzed the laboratory specimens tested in Natali Egorova's study (2014) using ABAQUS software to measure the accuracy, efficiency, and validity of the modeling method and analyze the specimens [19]. The results were then compared to determine to what extent software theoretical findings were consistent with practical laboratory findings. After developing a good modeling method and ensuring its validity, several software models of real dimensions with various parameters and variables were designed and examined to investigate the factors affecting the strength, stiffness, floor displacement, and energy dissipation of a wall. The specimens designed by Natalia Egorova et al. (2014) were provided and tested in smaller dimensions scaled from real specimens. As illustrated in Figure 1, the specimen is seen in a square form measuring 864 mm long with a net length of 762 mm.

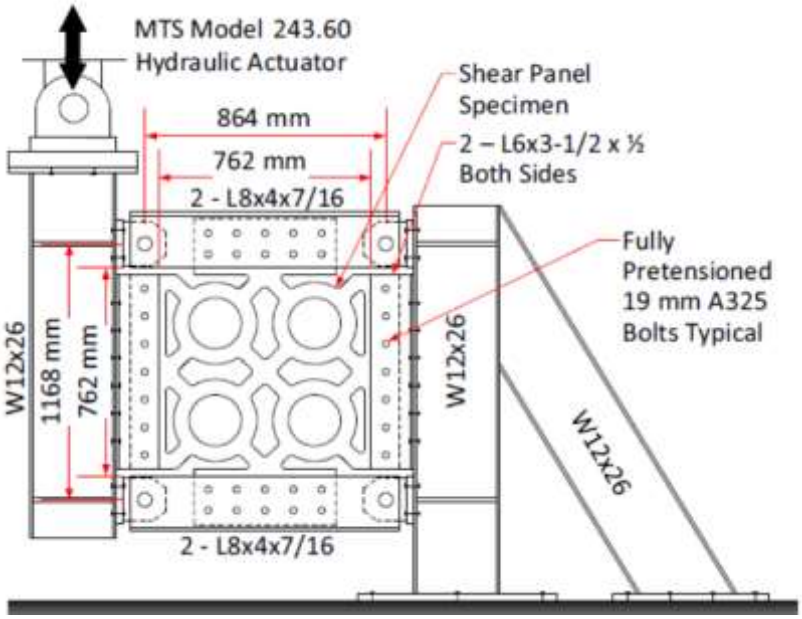

Figure 1: Schematic of the testing system [19]

Specimens designed based on laboratory specimens

In the study by Natalia Egorova et al. (2014), a total of 8 laboratory specimens were analyzed, with 6 specimens designed with ring-shaped steel plate shear wall patterns and analyzed for modeling in the software. Table 1 below gives the dimensional and non-dimensional specifications of these specimens. Also, a schematic of a ring-shaped steel plate shear wall is illustrated in Figure 2.

Table 1: Laboratory specimen data

	Specimen name	t (mm)	Ro (mm)	Wc (mm)	Wl (mm)	N	a/t	Ro/t	Wc/t
1	2-13-1	12.7	150	56	56.1	2	68	11.8	4.4
2	3-13-3	12.7	100	37.3	37.3	3	68	7.9	2.9
3	2-6-0.81	6.4	150	45.7	56.1	2	136	23.6	7.2

4	2-6-1	6.4	150	56.1	56.1	2	136	23.6	8.8
5	3-6-1	6.4	100	37.3	37.3	3	136	15.7	5.8
6	3-10-1	9.5	100	37.3	37.3	3	91	10.5	3.9

Where t is the sheet's thickness, R_O is the ring's outer radius, W_C is the ring's width, W_L is the connection link's width, N is the number of rings in each row, and a is the wall's width.

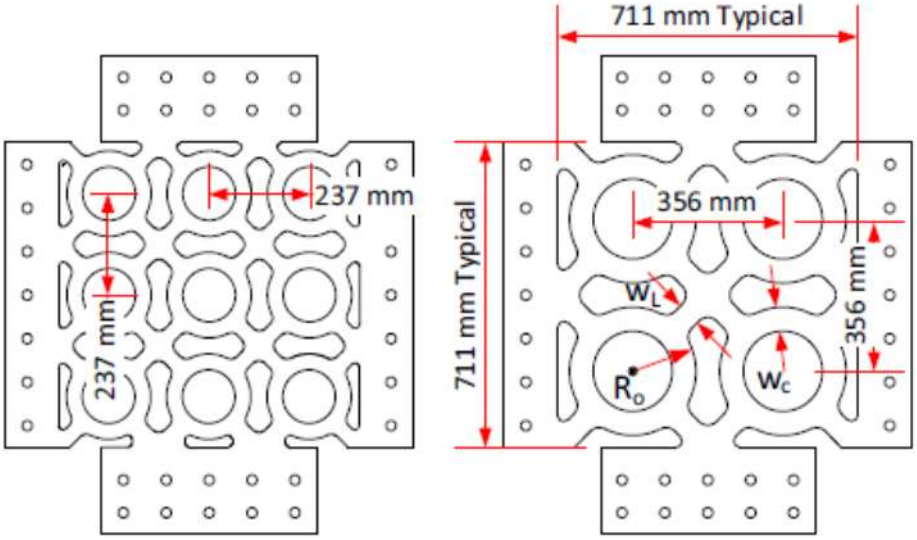

Figure 2: Schematic of laboratory specimens [19].

Software Model Sets

This section concerns all specimens designed and modeled in the software, as given by tables. Designed models are given in three sets with separate goals. Each table gives the effects of some special parameters.

Table 2: First set of software specimens

	t(mm)	Ro(mm)	Ro/Wc	Wc(mm)	Ro/W_L	W_L(mm)	Ro/t
A1	20	250	3.3	75.7	2	125	12.5
A2	16	250	3.3	75.7	2	125	15.63
A3	12	250	3.3	75.7	2	125	20.83

The following software specimens are mainly designed for investigating the effects of the ring's outer radius (R_O). In Table 2, the two parameters of R_O/W_L and R_O/W_C are assumed to be constant in all specimens, with other values varying by changing RO and t.

Table 3: Second set of software specimens

	t(mm)	*Ro (mm)*	*Ro/W_C*	*W_C (mm)*	*Ro/W_L*	*W_L (mm)*	*Ro/t*
B1	16	600	3.3	181	2	300	37.50

B2	20	400	3.3	121	2	200	20.00
B3	12	200	3.3	60	2	100	16.67
B4	20	600	3.3	181	2	300	30.00
B5	16	400	3.3	121	2	200	25.00
B6	20	200	3.3	60	2	100	10.00
B7	12	600	3.3	181	2	300	50.00
B8	12	400	3.3	121	2	200	33.33
B9	16	200	3.3	60	2	100	12.50

The following software specimens are mainly designed for investigating the effects of the parameters of R_O/W_C and R_O/W_L on the behavior of the wall.

Table 4: Third set of software specimens

	t(mm)	***Ro (mm)***	***Ro/W_C***	***W_C (mm)***	***Ro/W_L***	***W_L (mm)***	***Ro/t***
C1	20	250	2.5	100	2	125	12.50
C2	16	250	2.5	100	2	125	15.63
C3	12	250	2.5	100	2	125	20.83
C4	20	250	2	125	2	125	12.50
C5	16	250	2	125	2	125	15.63
C6	12	250	2	125	2	125	20.83
C7	20	250	3.3	75	1.5	166	12.50
C8	16	250	3.3	75	1.5	166	15.63
C9	12	250	3.3	75	1.5	166	20.83
C10	20	250	3.3	75	2.5	100	12.50
C11	16	250	3.3	75	2.5	100	15.63
C12	12	250	3.3	75	2.5	100	20.83
C13	20	250	3.3	75	3	83	12.50
C14	16	250	3.3	75	3	83	15.63
C15	12	250	3.3	75	3	83	20.83

Findings

Laboratory Specimens

In the first stage, laboratory specimens, tested by Egorova et al. in 2014, were modelled in the software to provide a specific and confirmed modeling method by adapting it to laboratory specimens.

Specimen 2-13-1

Figure 5-a gives a schematic of the dimensions of the ring-shaped steel plate shear wall. As noted, the wall is composed of four rings. In the software model, all the dimensions and thickness of the wall are applied without any changes. The unit of length is mm and the unit of force is kN. Figure 5-b illustrates the final buckling state in the software, which has yielded under the displacement of most of the points, with the buckling in the entire wall fully observable. The diagram illustrated in Figure 6-a shows the output of the software until the final displacement, while Figure 6-b shows the output of the specimens tested by Egorova et al. As noted, the maximum strength of laboratory specimens is 378 kN, while software specimens have a maximum strength of 333 kN. In initial cycles, there is an evident correspondence between software and laboratory models, but as the analysis suggests, stiffness degradation and strength degradation in the software model are more obvious than in the laboratory model. It is noteworthy that the continuation of the test in the laboratory model was not possible any longer due to the shear buckling in the frame, which caused the test to stop. In the software model, however, the software was capable of analyzing the specimen for up to 8% of the shear deformation, with the model going through all loading cycles.

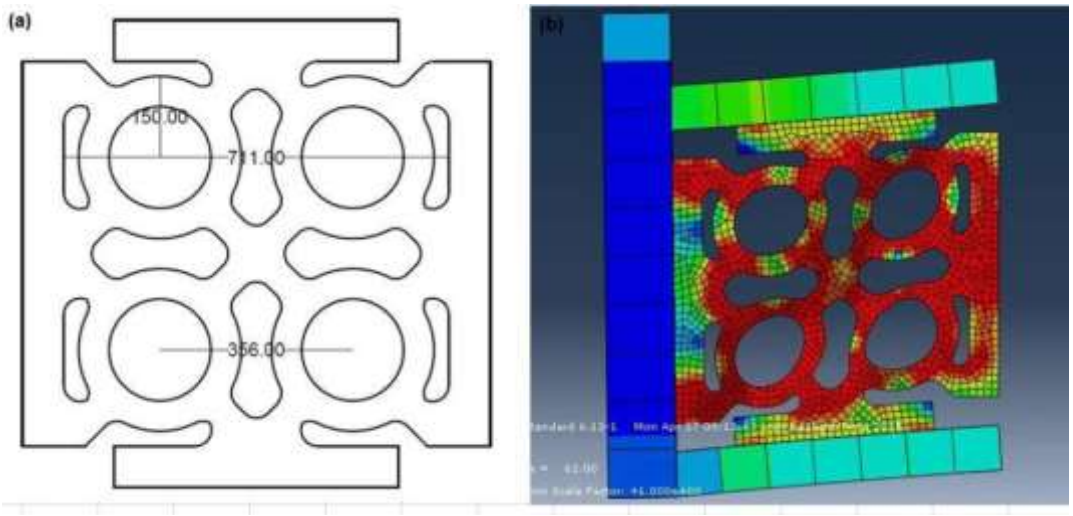

Figure 5: a) A view of the wall's dimensions and b) A view of the wall's buckling

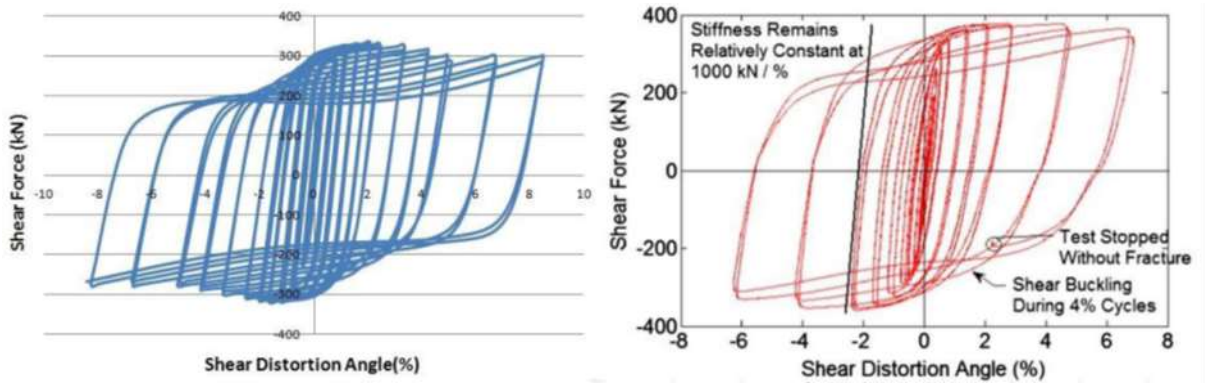

Figure 6: a) Hysteresis curve of software specimens and b) hysteresis curve of laboratory specimens

A comparison of all specimens in Table 5 reveals that there is a necessary match between laboratory and software specimens. It should be pointed out that because the exact figures and numbers of the practical test were not available and the laboratory specimens were not capable of applying all loading cycles, a comparison between the specimens based on the energy dissipated was not possible, either.

Specimen 3-13-1

This model includes 9 rings, and the distance and diameter of the rings and other specifications exactly are given in line with the laboratory model in the software. Figure 7-a illustrates a schematic of the wall and its state after buckling and at the endpoints of the test. Red dots in the figure show that a majority of the elements have reached yielding. The diagrams in Figure 7-b shows the output of the laboratory model. As noted, the testing of the model in regards to the shear deformation of 3% stopped due to frame fracture. Because other laboratory specimens usually suffered from strength degradation after shear deformation, the maximum shear strength of the test can be extracted from this specimen, which was 405 kN, as reported by the experimenter. Figure 8-a illustrates the output of the software model. Unlike laboratory specimens, the software was capable of going through all loading cycles and finishing the test. As illustrated, if loading cycles are considered at 3% shear deformation, no significant stiffness degradation or strength degradation will be noted, with the two diagrams largely matching each other. In subsequent loading cycles, however, stiffness degradation is fully evident after 3% shear deformation. The maximum strength of this laboratory model, as obtained from the software, was 407 kN. In general, good correspondence was noted between the laboratory model and the software model.

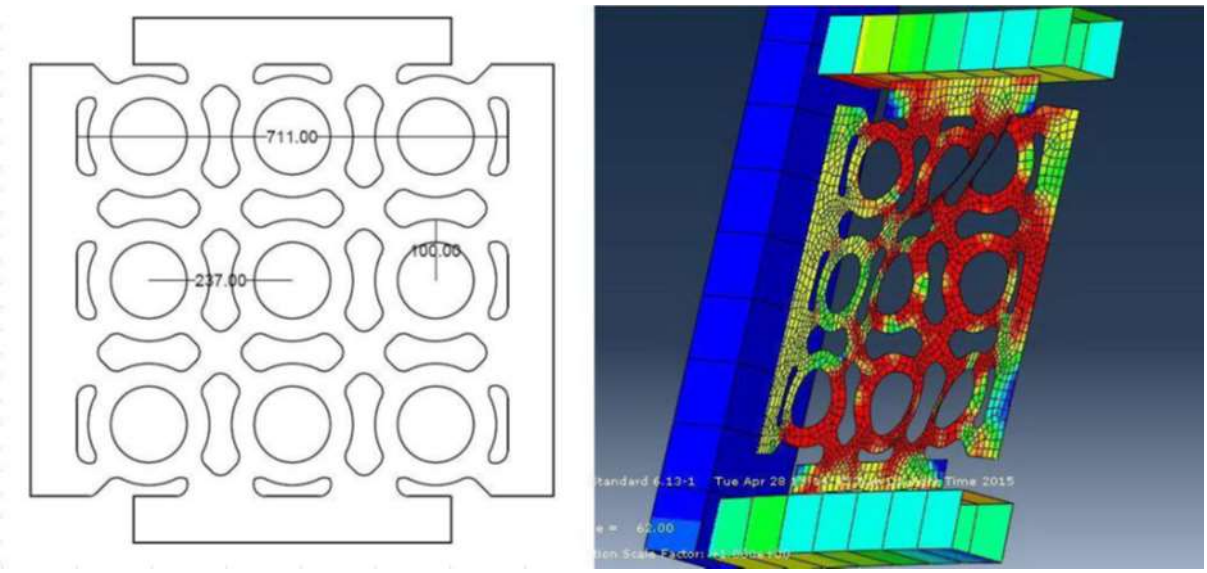

Figure 7: a) A view of the wall's dimensions, b) a view of the wall's buckling

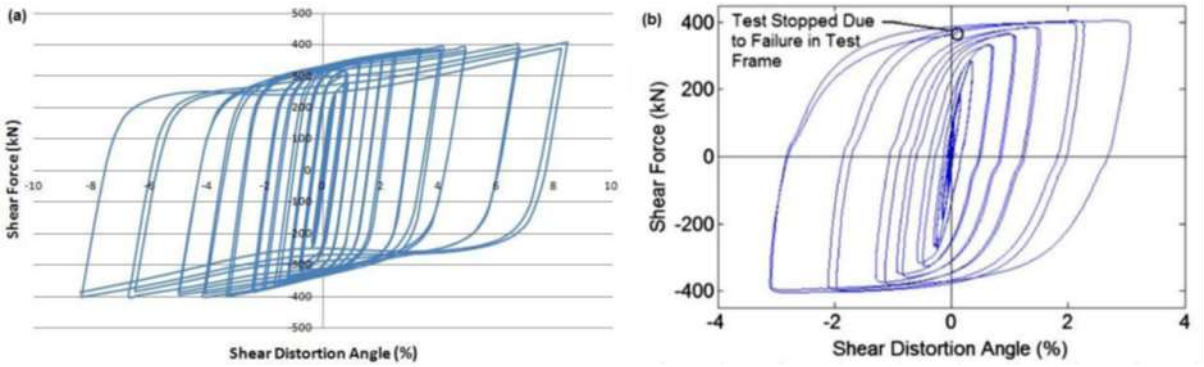

Figure 8: a) Hysteresis curve of the software specimen and b) hysteresis curve of the laboratory specimen

Table 5: Comparison of software and laboratory specimens

	Analysis model	Peak Strength	Strength Ratio (%)
2-13-1	**Exprimental**	**378**	**88.1**
	Software model	**333**	
3-13-3	**Exprimental**	**405**	**100.5**
	Software model	**407**	
2-6-0.81	**Exprimental**	**105**	**94.3**
	Software model	**99**	
2-6-1	**Exprimental**	**155**	**86.5**
	Software model	**134**	
3-6-1	**Exprimental**	**171**	**93.0**
	Software model	**159**	
3-10-1	**Exprimental**	**302**	**88.7**
	Software model	**268**	

Software Specimens

After arriving at a specific and validated method in prior stages, this section generalizes this method to a frame of real dimensions (about 5.5 m *3.5 m), while several specimens of various specifications are designed for investigating the effective factors, and modeled in the software using the stated method.

The C5 Model is a designed specimen. As seen in Figure 6, a schematic of the wall is illustrated. The wall measures around 6 m long and 3.5 m high. Because the size of the ring's diameter, thickness, etc. in each of the specimens varies, the length and height of the wall change by these parameters, though this change was less than 0.4 m; also, because single-ring specifications were used when comparing the models (e.g., total strength is divided by the number of rings to obtain single-ring strength) the change in length and height could not affect the final result.

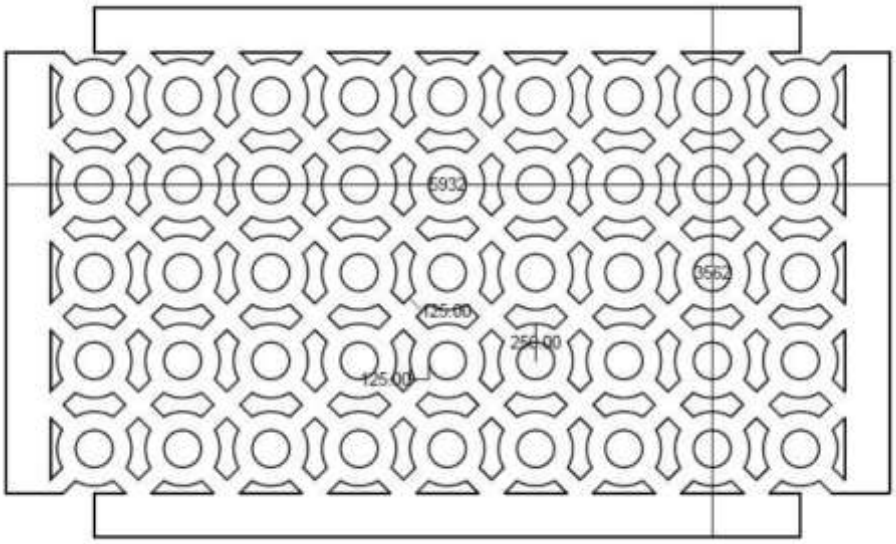

Figure 6: A view of the dimensions of the C5 ring-shaped steel plate shear wall

Figure 7 illustrates a ring-shaped steel plate shear wall modelled in a software workspace. This figure shows the view of the wall at the end of the loading. The colors of the wall also demonstrate the distribution of stress in the wall. As noted, stress is at its highest at the corners of the wall, with the diagonal line of the wall's buckling experiencing the highest stress. The diagonal form of the buckling has an almost 45° angle, and since the wall is rectangular, these two axes have not led to each other in the center of the wall.

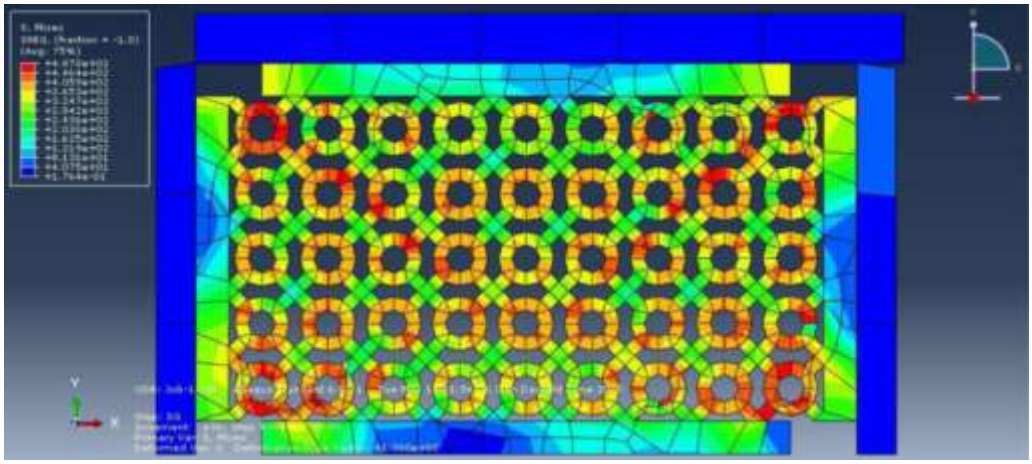

Figure 7: Stress distribution in the C5 specimen after the end of loading cycles

Figure 7 illustrates the way elements reach yielding. Red dots refer to regions wherein stress has crossed the yielding limit. This step is so selected to have the highest number of elements at the yielding point. This step is usually in the last cycle at the moment when the loading direction changes. The elements that withstand buckling fall under these yielded elements.

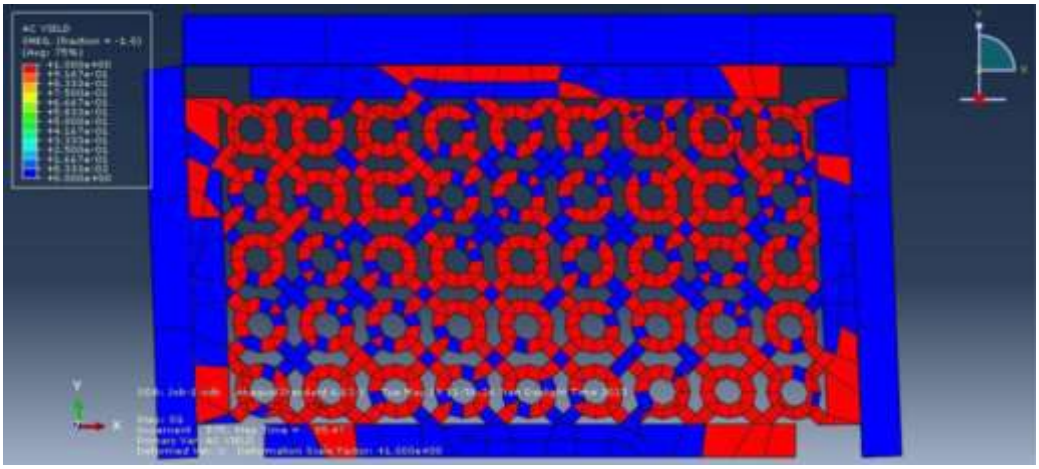

Figure 8: Elements that have crossed the yielding limit in the C5 specimen

Figure 9 illustrates the wall in a buckling state. As seen, the wall is wavy and experiences the highest stress at the buckling place, shown by red dots. It is noteworthy that buckling in the wall usually appears in the last cycles.

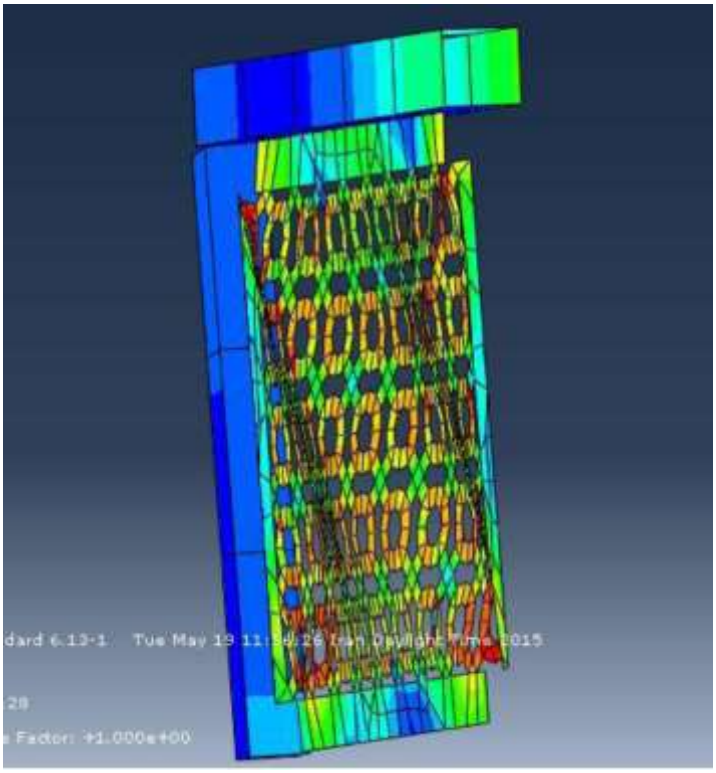

Figure 9: A view of the side wall in a buckling state

The diagrams in the figures illustrate the software outputs. The wall's support force is seen as the wall's reaction force. Displacement, as based on the loading protocol, has been applied to the free end of the upper beam at some time intervals.

Figures 10 and 11 illustrate the hysteresis diagram and the wall's uniform loading in one direction.

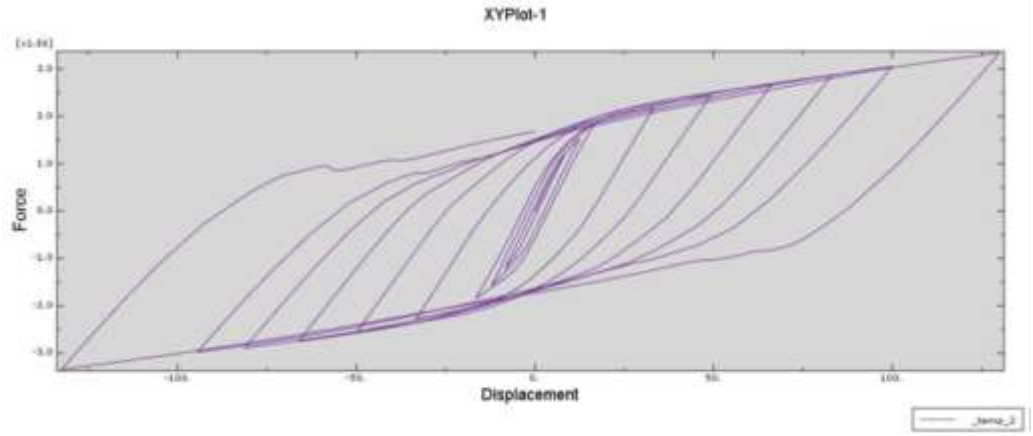

Figure 10: Hysteresis curve of the C5 specimen software output

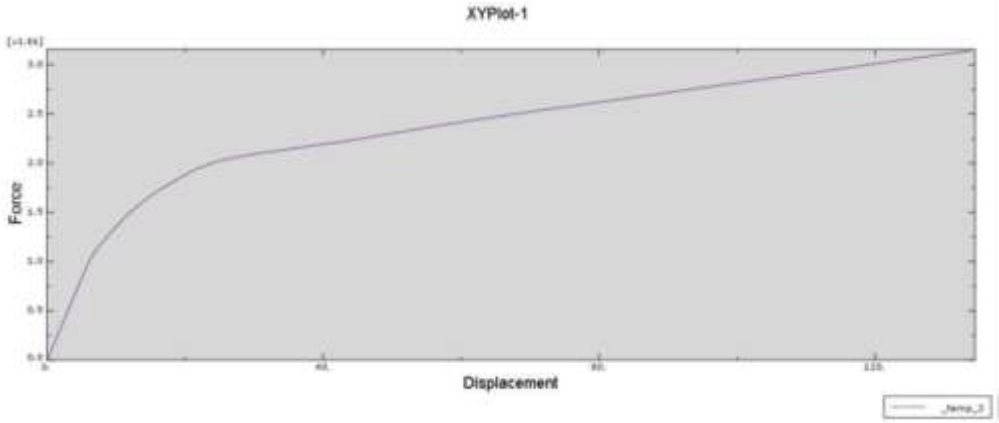

Figure 11: Force-displacement curve at the uniform state of the C5 specimen; software output

Tables 6, 7, and 8 give all results from laboratory specimens.

Table 9: Output parameters of the first group specimens

	STRENGTH (Kn)	*PEAK STRENGTH (Kn/mm)*	*STIFFNESS (Kn/mm)*	*YEILD DRIFT T(%)*	*ENERGY DISSIPATION (Kn-mm)*	*ENERGY DISSIPAION RATIO*
A1	1388	2240	56	0.70	218911	0.66
A2	1035	1538	41	0.71	130983	0.62
A3	715	1407	28	0.71	256974	0.73

Table 8: Output parameters of the second group specimens

	STRENGTH (Kn)	*PEAK STRENGTH (Kn/mm)*	*STIFFNESS (Kn/mm)*	*YEILD DRIFT T(%)*	*ENERGY DISSIPATION (Kn-mm)*	*ENERGY DISSIPAION RATIO*
B1	1131	1735	70	0.46	225974	0.62
B2	1631	3006	87	0.52	359741	0.75
B3	538	1092	25	0.49	74702	0.57
B4	1416	2292	93	0.43	335876	0.61
B5	1262	2122	72	0.49	208673	0.71
B6	913	2540	52	0.60	235820	0.64
B7	712	1427	69	0.36	170792	0.49
B8	637	1009	25	0.46	86339	0.49
B9	715	1730	37	0.54	141664	0.60

Table 9: Output parameters of the third group of specimens

	STRENGTH (Kn)	*PEAK STRENGTH (Kn/mm)*	*STIFFNESS (Kn/mm)*	*YEILD DRIFT T(%)*	*ENERGY DISSIPATION (Kn-mm)*	*ENERGY DISSIPAION RATIO*
C1	1472	3892	76	0.51	739147	0.79
C2	1113	2766	55	0.52	522844	0.80
C3	745	1723	37	0.52	334706	0.79
C4	2603	4291	207	0.35	926846	0.83
C5	1884	3347	165	0.32	711880	0.83
C6	1382	2420	108	0.36	487656	0.74
C7	1200	3142	97	0.35	395922	0.67
C8	956	2214	77	0.35	264842	0.57
C9	548	1460	55	0.28	143296	0.51
C10	988	2235	47	0.59	344596	0.82
C11	754	1568	35	0.60	232986	0.82
C12	531	1025	25	0.60	146790	0.78
C13	1008	2202	51	0.55	442802	0.83
C14	763	1586	39	0.54	314632	0.88
C15	528	1057	29	0.51	190110	0.81

Conclusion

Results indicated that the ring-shaped steel plate shear wall could remove the pinching effect in the hysteresis diagram of the simple ring-shaped steel plate shear wall and provide an acceptable hysteresis behavior. The removal of pinching in the hysteresis diagram caused the ring-shaped steel plate shear wall to demonstrate a higher rate of dissipated energy than the simple ring-shaped steel plate shear wall. The percentage of the dissipated energy compared to the ideal hysteresis diagram was around 75% in the ring-shaped steel plate shear wall, while that rate amounted to around 40% in the simple ring-shaped steel plate shear wall.

The effects of input parameters on the behavior and output parameters of the ring-shaped steel plate shear wall were obtained. As expected, it was possible to combine input parameters to separately adjust output parameters based on design needs in these ring-shaped steel plate shear walls.

The out-of-plane buckling in the ring-shaped steel plate shear wall was highly controlled, with the majority of the specimens experiencing no buckling in the first half of the loading cycles, as no stiffness or strength degradation was consequently seen.

It was found that an increase in thickness, a decrease in the ring's radius, an increase in the number of rings, and an increase in the ring's width could increase the strength in the ring-shaped steel plate shear wall. With the increase of thickness, decrease of the ring's radius, increase of the number of rings, increase of the connecting link's width, and increase of the ring's width, the stiffness of the ring-shaped steel plate shear wall also increased.

Also, an increase in thickness, a decrease in the width of the connecting link, and an increase in the ring's width helped increase the percentage of energy dissipated. As thickness relatively increased, the ring's radius decreased, and the ring's width increased, the relative displacement of the floor increased at the yielding limit.

In this study, software models had fully gone through loading cycles, whereas laboratory specimens had stopped in some states of the loading due to laboratory conditions. This is engendered in the lack of an accurate comparison of some parameters, including dissipated energy. For this, comparisons between diagrams were generally carried out.

Previous studies about steel plate shear walls indicated that the behavior of single-story, single-span frames was quite different from the behavior of multi-story, multi-span frames. As for steel plate shear walls, major findings are also expected. Also, the study of the behavior of walls on various floors paves the way for the use of these systems in practical projects, especially in structures in earthquake-prone areas.

References

[1] Jagtap RA, Gundecha SD, Shelar M, Gawade VS, Patil AA. 2-Hydroxyl Methacrylate based Triblock Copolymers by Atom Transfer Radical Polymerization. Int J Pharm Res Allied Sci. 2021;10(4):121-30.
[2] Karaderi S, Bayraktar S, Mazı C. UV-Visible Spectrophotometric Method for Complexes Stoichiometry between Zn(II), Mg(II), Cd(II), Ca(II) and Cu(II) with Clonidine Hydrochloride. Int J Pharm Res Allied Sci. 2021;10(3):83-8.
[3] Lubell, A., Prion, H., Ventura, C., Rezai, M., Unstiffened steel plate shear wall performance under cyclic loading, Journal of Structural Engineering (ASCE) 126 (4) (2000) 453-460.
[4] Schumacher, A., Grondin, G.Y., Kulak, G.L., Connection of infill panels in steel plate shear walls, Canadian Journal of Civil Engineering 26 (1992) 549-563.
[5] Berman, J.W., Celik, O.C., Bruneau, M., Comparing hysteretic behavior of light-gauge steel plate shear walls and braced frames, Engineering Structures 27 (3) (2005) 475-485.
[6] Chen, J.S., Jhang, C., Experimental study of low-yield-point steel plate shear wall under in-plane load, Journal of Construction Steel Research 67 (2011) 977-985.
[7] Tipping, S., B. Stojadinovic, S., Innovation corrugated steel shear walls for multi-story residential buildings, in: In proceeding of the 14th World Conference on Earthquake Engineering, 2008.
[8] Moghimi, H., Driver, R.G., Effect of regular perforation patterns on steel plate shear wall column demands, in proceedings of Structures Congress (ASCE), Las Vegas, Nevada, United States, 2011, pp. 2917-2928.
[9] Vian, D., Bruneau, M., Steel plate shear wall for seismic design and retrofit of building structures, MCEER Technical Report 05-0010, Multidisciplinary Center for Earthquake Engineering Research, University at Buffalo (2005).
[10] Hitaka, T., Matsui, C., Tsuda, K., Sadakane, Y., Elastic-plastic behavior of buildings of steel frame with steel bearing wall with slits, In proceeding of the 12th World Conference on Earthquake Engineering, no. 0833, Auckland, New Zealand, 2000.
[11] Hitaka, T. and Matsui, C., Experimental study on steel shear wall with slits, Journal of Structural Engineering (ASCE) 129 (5) (2003) 586-595.
[12] Ukibayev J, Datkhayev U, Myrzakozha D, Frantsev A, Karlova E, Nechepurenko Y, et al. Rectal methods of delivery of medical drugs with a protein nature in the therapies of tumor disease. J Adv Pharm Educ Res. 2021;11(1):18-22.
[13] Salih MRM, Abd AY. Knowledge, attitude, and behaviour regarding doping in sports among physicians and pharmacists: a questionnaire-based study. J Adv Pharm Educ Res. 2021;11(2):29-35.
[14] Cortes, G., Liu, J., Steel silt panel configurations, In proceeding of the 14th World Conference on Earthquake Engineering, Beijing, China, 2008.
[15] Borchers, E., Pena, A., Krawinkler, H., Deierlein, G., Design and behavior of steel shear plates with opening as energy-dissipating fuses, Internal report, Blume Earthquake Engineering Center, Stanford University, Stanford, California (2010).
[16] Sadovnikova NA, Lebedinskaya OG, Bezrukov AV, Davletshina LA. The indicator system of regional socio-economic situation based on harmonized information resources. J Adv Pharm Educ Res. 2021;11(1):147-55.

[17] Tyler, R.G., Further notes on a steel energy-absorbing elements for braced frameworks, Bulletin of the New Zealand National Society for Earthquake Engineering 18 (3) (1985) 270-279
[18] Ciampi, V., Samuelli-Ferretti, A., Energy dissipation in buildings using special bracing systems, In proceedings of the 9th European Conference on Earthquake Engineering, Vol. 3 of 9-18, Moscow, Russia, 1990.
[19] Egorova N., Eatherton M.R., Maurya A., Experimental study of ring-shaped steel plate shear walls, Journal of Constructional Steel Research 103 (2014) 179–189